Modelling of gaseous methylamines in the global atmosphere: Impacts of oxidation and aerosol uptake

Fangqun Yu* and Gan Luo

Atmospheric Sciences Research Center, State University of New York, 251 Fuller Road, Albany, New York 12203, USA

*corresponding author: fyu@albany.edu

Abstract. Gaseous amines have attracted increasing attention due to their potential role in enhancing particle nucleation and growth and affecting secondary organic aerosol formation. Here we study with a chemistry transport model the global distributions of the most common and abundant amines in the air: monomethylamine (MMA), dimethylamine (DMA), and trimethylamine (TMA). We show that gas phase oxidation and aerosol uptakes are dominant sinks for these methylamines. The oxidation alone (i.e., no aerosol uptake) leads to methylamine lifetimes of 5-10 hours in most parts of low and middle latitude regions. The uptake by secondary species with uptake coefficient (γ) of 0.03 (corresponding to the uptake by sulfuric acid particles) reduces the lifetime by ~30% over oceans and much more over the major continents, resulting in methylamine lifetime of less than 1-2 hours over central Europe, East Asia, and Eastern US. With the estimated global emission flux, from the reference, our simulations indicate that [DMA] in the model surface layer over major continents is generally in the range of 0.1 – 2 ppt when γ = 0.03 and 0.2-10 ppt when γ = 0, and decreases quickly with altitude. [DMA] over oceans is below 0.05 ppt and over polar regions is below 0.01 ppt. The simulated [MMA] is about a factor of ~2.5 higher while [TMA] is a factor of ~ 8 higher than [DMA]. The modeled concentrations of methylamines are substantially lower than the limited

25 observed values available, with normalized mean bias ranging from -57% ($\gamma = 0$) to -88% ($\gamma =$
26 0.03) for MMA and TMA, and -78% ($\gamma = 0$) to -93% ($\gamma = 0.03$) for DMA.
27

1. Introduction

In recent years, gaseous amines have attracted increasing attention due to theoretical, laboratory, and field measurements indicating that amines may considerably enhance particle formation and growth (Kurten et al., 2008; Nadykto et al., 2011, 2014; Almeida et al., 2013; Berndt et al., 2010; Zhao et al., 2011; Erupe et al., 2011; Chen et al., 2012; Wang et al., 2010; Yu et al., 2012) and affect secondary organic aerosol (SOA) formation (De Haan et al., 2009, Myriokefalitakis et al., 2010; Williams et al., 2010). Amines are organic compounds and derivatives of ammonia wherein one or more hydrogen atoms are replaced by a substituent such as an alkyl or aryl group. About 150 amines have been identified in the atmosphere; the most common and abundant amines being the low-molecular-weight methylamines like monomethylamine (MMA), dimethylamine (DMA), and trimethylamine (TMA) (Ge et al., 2011a). Concentrations of amines can exceed several parts-per-billion-volume (ppbv) near their sources (Ge et al., 2011a; Schade and Crutzen, 1995) but are expected to be low farther away as a result of their short lifetime due to oxidation by OH (Carl and Crowley, 1998) and uptake by particles (Qiu and Zhang, 2013).

While amines are stronger bases than ammonia and ternary H_2SO_4-H_2O-amine clusters are more stable (Kurten et al., 2008; Nadykto et al., 2011, 2014; Almeida et al., 2013), the relative role of amines versus ammonia in enhancing particle formation in the atmosphere is yet to be determined (Zollner et al., 2012). This is because the concentration of amines in the atmosphere is generally much lower than that of ammonia (by 2-3 orders of magnitude or more) (Ge et al., 2011a; Hanson et al., 2011). Recent measurements taken during the CLOUD (Cosmics Leaving Outdoor Droplets) chamber experiments at CERN (Almeida et al., 2013) indicate that a [DMA]

of above ~ 5 parts-per-trillion-volume (pptv) enhances nucleation substantially, but enhancement drops significantly as [DMA] decreases below that level.

In order to determine the contribution of ternary nucleation involving amines to atmospheric particle production, it is critical to know the concentrations of key amines and their variations in the atmosphere. Due to their high reactivity and low concentrations, measurements of gaseous amines in the background atmosphere are very limited (Ge et al., 2011a). Several studies show [DMA] is below 1 pptv in urban areas (Grönberg et al., 1992a, b) while a couple of other studies observed [DMA] around a few pptv in rural and coastal areas (Hanson et al., 2011; VandenBoer et al., 2011, 2012; Van Neste et al., 1987; Gibb et al., 1999). Although TMA is generally more abundant (Ge et al., 2011a), the concentration of TMA needed to substantially enhance nucleation remains to be studied.

In addition to in-situ measurements, numerical modeling is also needed to integrate the various processes controlling amine concentrations and ultimately assess the impact of amines on global nucleation, aerosol properties, and climate. While limited measurements of amines are available, modeling of global amines is basically non-existent. Myriokefalitakis et al. (2010) explored the potential contribution of amines emitted from oceans to the SOA formation, assuming total amines emissions to be one tenth of the oceanic ammonia emissions. Myriokefalitakis et al. (2010) neither considered amines from continental sources nor presented concentrations of gaseous amines over oceans. In the present work, we aim to simulate the global distributions of gaseous amines in the air with a global chemistry transport model. The key processes controlling amine concentrations (including emission, transport, oxidation, deposition, and aerosol uptake) are considered and the simulated results are compared to the limited measurements available.

The methods of the present study (including sources, sinks, and model representation) are described in Section 2. The modeling results, comparisons with measurements, and sensitivity studies are given in Section 3. Section 4 is the summary and discussion.

2. Methods

2.1. Sources and fluxes

Amines are ubiquitous atmospheric organic bases, and are emitted from a wide range of sources including animal husbandry, biomass burning, motor vehicles, industry, meat cooking, fish processing, sewage treatment and waste incineration, protein degradation, vegetation, soils, and ocean organisms (Ge et al., 2011a). On a global scale, little is known about the flux of most amines, especially various aromatic amines (Ge et al., 2011a). Among about 150 amines identified in the atmosphere, methylamines (MMA, DMA, and TMA) are most common and abundant. Schade and Crutzen (1995) estimated the global emission fluxes of MMA, DMA, and TMA to be 83±26, 33±19, and 169±33 Gg N yr^{-1}, respectively. The total methylamine flux of 285±78 Gg N yr^{-1} is more than two orders of magnitude smaller than the estimated global ammonia flux of 50000±30000 Gg N yr^{-1} (Schade and Crutzen, 1995).

2.2. Sinks

The main sinks of amines emitted into the atmosphere include dry and wet deposition, gas phase reactions, and heterogeneous uptake. Since most of the amines are highly soluble, wet deposition is an important process to bring amines in the air to the surface. As organic compounds, gaseous amines undergo oxidation reactions with OH, NO_x, or O_3 (Nielsen et al., 2012; Lee and Wexler, 2013). The lifetimes of amines with respect to OH oxidation are typically a couple of hours, much shorter than those by reactions with O_3 and NO_x. The gaseous

methylamines, which are strong bases, may also undergo rapid acid-base reactions to form salt particles in the presence of inorganic acids (HCl, HNO_3, H_2SO_4) (Murphy et al., 2007). In addition, amines may react with organic acids to form amides (Barsanti and Pankow, 2006). A detailed discussion of the chemistry of amines in the atmosphere can be found in several recent review articles (Nielsen et al., 2012; Lee and Wexler, 2013).

Owing to their high aqueous solubility and strong basicity, gaseous amines can efficiently enter into a particulate phase via direct dissolution and acid-base reactions. The importance of amines with regard to gas/particle partitioning has been supported by the reactive uptake of TMA into ammonium nitrate particles (Lloyd et al., 2009) and amine exchange into ammonium bisulfate and nitrate nuclei (Bzdek et al., 2010). Laboratory studies show that heterogeneous reactions of gaseous alkylamines on H_2SO_4 nanoparticles resulted in the formation of alkyl ammonium sulfates and particle growth (Wang et al., 2010a, b). It has also been observed that methylamine could react with glyoxal in drying cloud droplets to form SOA (De Haan et al., 2009) and stable aminium salts could be formed by amine and organic acids in the aerosols (Williams et al., 2010). The thermodynamic properties of amines that control their partitioning between the gas and the particle phase in the atmosphere are examined in a review paper (Ge et al., 2011b). An overview of laboratory progress in the multiphase chemistry of amines can be found in Qiu and Zhang (2013).

2.3. Model representation

A numerical model is needed to integrate the various processes influencing the concentrations of amines in the atmosphere. In the present study, we employ GEOS-Chem, a global 3-D model of atmospheric composition driven by assimilated meteorological data from the NASA Goddard Earth Observing System 5 (GEOS-5) (e.g., Bey et al., 2001). The GEOS-

Chem model has been developed and used by many research groups and contains a number of state-of-the-art modules treating various chemical and aerosol processes with up-to-date key emission inventories (for details, see the model webpage http://geos-chem.org/). Global ammonia emissions are based on the inventory developed by the Global Emission Inventory Activity (GEIA) (Bouwman et al., 1997) and national emission estimates are used for the US (NEI05), Canada (CAC), Europe (EMEP), and East Asia (Streets2000). While ammonia is simulated in detail in GEOS-Chem, amines are not considered prior to this study. Here, to represent gas phase methylamines, we add three tracers (MMA, DMA, and TMA) in GEOS-Chem V8.3.2 with an advanced particle microphysics (APM) model incorporated (Yu and Luo, 2009).

There exist large uncertainties in the estimated emission fluxes of amines and detailed emission inventories of amines from various sources are currently not available. In the present study, we use the ratios of methylamines to ammonia fluxes given in Schade and Crutzen (1995) but approximate the spatial distribution and seasonal variations of amine emissions following those of ammonia. Such a first order approximation enables us to simulate the typical concentrations of amines in the global atmosphere. The dry and wet deposition, as well as horizontal and vertical transport of amines, is also considered in GEOS-Chem, following the approaches for ammonia.

In the present study, we only take into account the oxidation of methylamines by OH as the oxidation of amines by NO_3 and O_3 is much smaller. There have been limited measurements of the kinetics of OH reactions with simple alkyl amines (Ge et al., 2011a; Nielsen et al., 2012; Lee and Wexler, 2013). In this study we use the reaction coefficients reported by Carl and Crowley (1998): 1.79×10^{-11}, 6.49×10^{-11}, and 3.58×10^{-11} cm^3 $molecule^{-1}$ s^{-1}, for MMA, DMA, and TMA,

respectively. For comparison, the reaction coefficient of NH_3 with OH is 1.6×10^{-13} cm^3 $molecule^{-1}$ s^{-1} (Atkinson et al., 1997), more than two orders of magnitude smaller. The uptake of amines by particles is considered, using the particle surface areas calculated from particle size distributions predicted by GEOS-Chem-APM. One key uncertainty about the heterogeneous uptake is the uptake coefficient (γ), defined as the ratio of gas surface collisions that result in loss of the amines onto the surface to the total gas surface collisions. Lloyd et al. (2009) reported a reactive uptake coefficient of 2×10^{-3} for the uptake of TMA by ammonium nitrate aerosols at 20% RH. Wang et al. (2010b) studied the uptake of alkylamines (MMA, DMA and TMA) on sulfuric acid surfaces and found uptake coefficients in the range of (2.0–4.4) $\times10^{-2}$. In a laboratory study of the heterogeneous reactions between alkylamines (MMA, DMA and TMA) and ammonium salts (ammonium sulfate and ammonium bisulfate), Qiu et al. (2011) found that, for the three alkylamines, the initial uptake coefficients (γ_0) range from 2×10^{-2} to 3.4×10^{-2} and the steady-state uptake coefficients (γ_{ss}) range from 6.0×10^{-3} to 2.3×10^{-4} and decrease as the number of methyl groups on the alkylamine increases. It is clear from these laboratory studies that the values of γ depend on the particle compositions. The secondary components of particles in the atmosphere (sulfate, nitrate, SOA, and ammonium), which are likely to play an important role in the uptake of amines, are generally internally mixed. The uptake coefficients of amines by these mixed particles, under different atmospheric conditions (especially RH), are not yet known. In the present study, the sensitivity of predicted amine concentrations to γ values ranging from 0 (no uptake) to 0.03 is studied. We assume no uptake of amines by pure dust, black carbon, and primary organic carbon. We do not consider the uptake of amines by sea salt particles due to lack of information with regard to the uptake coefficients. The gaseous phase reactions of amines with HNO_3, HCl, and organic acids are not considered, since oxidation and aerosol uptake likely

dominate the loss of amines. In the present study, we also do not consider the re-evaporation of amines after uptake by secondary particles as laboratory studies indicate that amines can react with various acids to form stable aminium salts (e.g., Qiu and Zhang, 2013). For example, recent laboratory measurements show that sulfate particles act as an almost perfect sink (negligible evaporation) for amines (Almeida et al., 2013).

3. Results

The results presented below are based on a one-year simulation (10/2005-12/2006, with the first 3 months as spin-up) using GEOS-Chem v8-03-02 + APM, with the kinetic condensation of low volatile secondary organic gases from successive oxidation aging taken into account (Yu, 2011). The horizontal resolution (latitude by longitude) is $2^o \times 2.5^o$ and there are 47 vertical layers in the model (surface to 0.01 hpa).

Table 1 shows global annual mean emissions, sinks (due to oxidation, uptake, and dry/wet deposition), and burdens for ammonia, MMA, DMA, and TMA. Sinks and burdens of methylamines under four different uptake coefficients (γ = 0.03, 0.01, 0.001, and 0) are given. Global ammonia emission flux for 2006 based on GEOS-Chem is 5.8×10^4 Gg N yr^{-1}, about 15% higher than the estimation of Schade and Crutzen (1995). The MMA, DMA, and TMA emissions fluxes assumed in the present study (96.2, 38.3, and 196.0 Gg N yr^{-1}, respectively) are also 15% higher, as the same ratios of methylamines to ammonia emission fluxes given in Schade and Crutzen (1995) are used. The 15% difference is within the estimated methylamines emissions uncertainty of ~ 30% (Schade and Crutzen, 1995).

As an example for the spatial distribution of emission fluxes, Figure 1 presents the horizontal distributions of DMA emissions assumed in the present study. As mentioned earlier, we

188 approximate the spatial distribution and seasonal variations of methylamines emissions following
189 those of ammonia. Again, this should be considered as a first order approximation, as the
190 emission rates of amines from various sources may be quite different from those of ammonia.
191 With the understanding of this limitation, we can see from Figure 1 that DMA emission rates are
192 in the range of ~ 0.2 to 10 kg N $km^{-2}yr^{-1}$ over major continents and below 0.2 kg N $km^{-2}yr^{-1}$ over
193 oceans. For MMA and TMA, the absolute emission fluxes are a factor of 2.5 and 5.1 higher
194 (Table 1). In Figure 1 we also marked the locations of sites where some kind of methylamines
195 measurements are available, as summarized in Table 2. It should be noted that sites A, B, D, and
196 G are close to each other and overlap in Figure 1. Similarly, sites E and F overlap in Fig. 1. Sites
197 J and K are the same location but measurements were taken during different time periods. A
198 comparison of simulated and observed methylamines concentrations is discussed later.
199 It can be seen from Table 1 that gas phase oxidation and aerosol uptakes are dominant sinks
200 for methylamines (Table 1). As expected, the uptake sinks are sensitive to uptake coefficients (γ)
201 when $\gamma > \sim 0.001$ and the oxidation becomes more important when γ is smaller. The change of γ
202 from 0.03 to 0.001 increases the modeled global burdens of methylamines by a factor of ~ 2.7.
203 Further decrease of γ from 0.001 to 0 has relatively small effects on the predicted burdens. Dry
204 and wet deposition accounts for 11-14% and 25-35% of the sinks when γ=0.03 and γ=0,
205 respectively. The global burdens of MMA, DMA, and TMA are respectively from 0.07 to 0.27
206 Gg N, 0.03 to 0.08 Gg N, and 0.24 to 0.72 Gg N as γ changes from 0.03 to 0. The ratios of
207 ammonia burden to that of methylamines (MMA+DMA+TMA) range from 74 (γ=0) to 236
208 (γ=0.03). The burdens are roughly but not strictly proportional to emission fluxes because of the
209 difference in the oxidation rates and deposition velocities (which also depend on molecular
210 weights).

Figure 2 shows the simulated horizontal distributions of annual mean DMA oxidation and uptake lifetime (τ, calculated as the ratio of the burden in each gird box to the corresponding sinks associated with oxidation and uptake) and concentration ([DMA]) in the model surface layer (0-150 m above surface) under two aerosol uptake coefficients: (a-b) γ=0 (i.e., oxidation only) and (c-d) γ=0.03 (uptake by sulfuric acid particles). The corresponding zonally averaged vertical distributions of τ and [DMA] are given in Figure 3. The oxidation only condition (i.e., no aerosol uptake) leads to a DMA lifetime of 5-10 hours in most parts of lower and middle latitude regions, from the surface to the upper troposphere. The oxidation lifetime is relatively long (from 10 to > 200 hours) over the high latitude regions due to low OH concentrations there. The aerosol uptake with γ=0.03 (upper limit, corresponding to the uptake by sulfuric acid particles) shortens the lifetime of DMA by ~30% over oceans and much more over the major continents, resulting in a DMA lifetime less than 1-2 hours over central Europe, east Asia, and the eastern US (Fig. 2c). Our sensitivity study indicates that τ values decrease with increasing γ when $\gamma > 0.001$ but become relatively insensitive to γ when $\gamma < 0.001$, as oxidation dominates the lifetime under this condition.

As a result of short lifetime, high values of [DMA] are generally confined to the source regions (Figs. 1, 2b, 2d). Depending on the uptake coefficients, [DMA] in the surface layer over major continents is in the range of 0.1 – 2 ppt when $\gamma = 0.03$ (Fig. 2d) and 0.2 – 10 ppt when $\gamma = 0$ (Fig. 2b). [DMA] decreases quickly with altitudes, with zonally averaged values dropping below 0.1 ppt a few hundred meters above the surface (Figs. 3b, 3d). [DMA] over oceans are below 0.05 ppt and these DMA are emitted from marine organisms (Fig. 1) rather than transported from continents. [DMA] over polar regions is below 0.01 ppt (Figs. 2 & 3) due to the lack of emissions there (Fig. 1).

234 The annual mean horizontal and vertical distributions of MMA and TMA concentrations
235 ([MMA], [TMA]) under two γ values (0.03, and 0) are shown in Figures 4 and 5. As a result of
236 same emission spatial distributions (assumed) and short lifetimes, [MMA] and [TMA] have
237 similar spatial distributions as those of [DMA]. [MMA] is generally a factor of ~2.5 higher than
238 [DMA], reaching 0.2 – 5 ppt when $\gamma = 0.03$ (Fig. 4c) and 0.5 – 20 ppt when $\gamma = 0$ (Fig. 4a) in the
239 surface layer over major continents. While the oxidation rate of MMA is smaller than that of
240 DMA, its deposition velocity is larger. As a result, [MMA] to [DMA] ratio is close to the ratio of
241 the corresponding global emission fluxes. In contrast, both oxidation and deposition velocity of
242 TMA is smaller than those of DMA, leading to a larger [TMA] to [DMA] (~ 8) than the
243 corresponding ratio of emission fluxes (~ 5). [TMA] in the surface layer over major continents
244 reaches 1 – 10 ppt when $\gamma = 0.03$ (Fig. 5c) and 2 – 50 ppt when $\gamma = 0$ (Fig. 5a). Similar to
245 [DMA], [MMA] and [TMA] decrease quickly with altitudes, down to < 0.1 ppt above ~ 800 mb
246 (Figs. 4b, 4d, 5b, and 5d).

247 Figure 6 compares the simulated [MMA], [DMA], and [TMA] with measurements at the
248 sites listed in Table 2 and marked in Fig. 1. The modeling results under four γ values (0.03, 0.01,
249 0.001, and 0) are given. It should be noted that the model results in Figs. 2-5 are annual mean
250 values, while most of the methylamines data are from various field measurements that lasted
251 from less than one day to a few months (Table 2). Owing to large seasonal variations, model
252 results corresponding to the months of the observations are used for comparisons with
253 observations in Fig. 6. The vertical bars in Fig. 6 (for γ=0.03 and 0 cases only) define the
254 simulated ranges of monthly mean concentrations of methylamines.

255 Based on very limited measurements currently available (Table 2), [DMA] in urban areas is
256 smaller than while [MMA] and [TMA] are close to those in rural and coastal areas. Over the

Arabian Sea, measurements of two periods differ by a factor of 5 for [DMA] and by a factor of 10 for [TMA], indicating a large temporal variation in [DMA] and [TMA] concentrations at some locations. It is clear from Figure 6 that the model predictions of methylamines are substantially lower than the limited observed values available, with normalized mean bias (NMB) ranging from -57% ($\gamma = 0$) to -88% ($\gamma = 0.03$) for MMA and TMA, and -78% ($\gamma = 0$) to -93% ($\gamma = 0.03$) for DMA. [MMA] and [TMA] are relatively closer to observed values, especially when $\gamma<\sim0.001$. It appears that the simulated [DMA] are close to the measured values for the three urban sites (A, B, and C) (Fig. 6b).

It is unclear how much the underestimation is associated with the spatial (2^{o}x2.5^{o} model grid box with a depth of ~ 150 m versus measurements at given sites near surface) and temporal (model monthly mean versus measurements of a few days to a few weeks) average. The seasonal variations of simulated concentrations of methylamines are generally within a factor of 2 – 5. As we can see from Figs. 2-5 and Table 1, concentrations of methylamines are roughly proportional to the emission fluxes. Methylamines emissions in certain regions could be much larger while, in other regions, much lower than those shown in Fig. 1. Due to the short lifetime of these amines, long range transport is not important, thus the observed amines concentrations (together with their lifetime) can be used to estimate the emission strength in the region. If the measurements are representative and reflect the real methylamines concentrations, the under-prediction of methylamines by one to two orders of magnitude in some sites (Fig. 6) may indicate that the methylamines emissions in these regions are one to two orders of magnitude larger than those assumed in this study (Fig. 1 and Table 1), at least around the sites of the measurements. Apparently long-term measurements of amines at more locations are needed to evaluate the potential importance of amines.

4. **Summary and discussion**

As a result of the substitution by one or more organic functional groups, amines have stronger basicity than ammonia and may participate in new particle formation in the atmosphere. To integrate the various processes controlling amines concentrations and understand the concentrations of key amines and their spatiotemporal variations in the atmosphere, we simulate the global distributions of amines in the air with a global chemistry transport model (GEOS-Chem), focusing on methylamines (MMA, DMA, and TMA) in this study.

We showed that gas phase oxidation and aerosol uptakes are dominant sinks for methylamines. The uptake sinks are sensitive to uptake coefficients (γ) when $\gamma > \sim 0.001$ and the oxidation becomes more important when γ is smaller. The oxidation only (i.e., no aerosol uptake) leads to a methylamines lifetime of 5-10 hours in most part of low and middle latitude regions, from the surface to the upper troposphere. The oxidation lifetime is relatively longer (> 10-50 hours) over the high latitude regions due to low OH concentrations there. The aerosol uptake with uptake coefficient (γ) of 0.03 reduces the lifetime of methylamines by ~30% over oceans and much more over the major continents, resulting in methylamines lifetime as short as 1-2 hours over central Europe, East Asia, and Eastern US. Depending on γ values, [DMA] in the surface layer over major continents is in the range of 0.1 – 2 ppt when $\gamma = 0.03$ and 0.2 – 10 ppt when $\gamma = 0$, much smaller over oceans are polar regions (< 0.01 – 0.05 ppt). Compared to [DMA], [MMA] is generally a factor of ~2.5 higher while [TMA] is a factor of ~ 8 higher. Concentrations of methylamines decrease quickly with altitudes, with zonally averaged values dropping below 0.1 ppt above the boundary layer.

The simulated concentrations of methylamines are substantially lower than the limited observed values available, with normalized mean bias (NMB) ranging from -57% (γ = 0) to -88% (γ = 0.03) for MMA and TMA, and -78% (γ = 0) to -93% (γ = 0.03) for DMA. The underestimation can't be explained by the possible uncertainty in the uptake coefficients and long range transport. The concentrations of methylamines are roughly proportional to their emission fluxes, and thus the model under-prediction by one to two orders of magnitude at some sites may indicate that the methylamines emissions in these regions are one to two orders of magnitude higher than those assumed in this study. It should be noted that methylamines measurements are very limited and subject to large uncertainty as well because of their low concentrations and short lifetime.

Amines have been suggested to be the most likely compound to sequester carbon dioxide and there exists concern about the potential impacts of substantial increases in future amine emissions (Nielsen et al., 2012). Our study indicates that the impact of amine emissions from carbon sequestration is likely to be local rather than global as a result of their short lifetime. The low concentrations of amines away from source regions (<0.1-1 ppt) suggest that the impact of amines on global new particle formation may be quite limited. Nevertheless, amines can exceed a few ppt over the main source regions and thus may substantially enhance new particle formation. It should be noted that about 150 amines have been identified in the atmosphere and amines of different kinds are likely to have different abilities in stabilizing pre-nucleation clusters. It is important to identify those amines with abundant concentrations in the atmosphere and study their ability in enhancing new particle formation. We would like to emphasize that the present global simulations of methylamines are subject to uncertainties associated with emissions, uptake coefficients, and chemistry. Further laboratory study, field measurement, and

numerical modeling are needed to advance our understanding of spatiotemporal distributions of key amines and to evaluate their contributions to new particle formation and growth in the global atmosphere.

Acknowledgments. This study was supported by NASA under grant NNX13AK20G. The GEOS-Chem model is managed by the Atmospheric Chemistry Modeling Group at Harvard University with support from NASA's Atmospheric Chemistry Modeling and Analysis Program.

References

Almeida J, Schobesberger S, Kürten A, Ortega IK, Kupiainen-Määttä O, Praplan AP, Adamov A, Amorim A, Bianchi F, Breitenlechner M, David A, Dommen J, Donahue NM, Downard A, Dunne E, Duplissy J, Ehrhart S, Flagan RC, Franchin A, Guida R, Hakala J, Hansel A, Heinritzi M, Henschel H, Jokinen T, Junninen H, Kajos M, Kangasluoma J, Keskinen H, Kupc A, Kurtén T, Kvashin AN, Laaksonen A, Lehtipalo K, Leiminger M, Leppä J, Loukonen V, Makhmutov V, Mathot S, McGrath MJ, Nieminen T, Olenius T, Onnela A, Petäjä T, Riccobono F, Riipinen I, Rissanen M, Rondo L, Ruuskanen T, Santos FD, Sarnela N, Schallhart S, Schnitzhofer R, Seinfeld JH, Simon M, Sipilä M, Stozhkov Y, Stratmann F, Tomé A, Tröstl J, Tsagkogeorgas G, Vaattovaara P, Viisanen Y, Virtanen A, Vrtala A, Wagner PE, Weingartner E, Wex H, Williamson C, Wimmer D, Ye P, Yli-Juuti T, Carslaw KS, Kulmala M, Curtius J, Baltensperger U, Worsnop DR, Vehkamäki H, Kirkby J.: Molecular understanding of sulphuric acid–amine particle nucleation in the atmosphere, Nature, 502, 359-363, 2013.

Atkinson, R., Baulch, D.L., Cox, R.A., Hampson Jr., R.F., Kerr, J.A., Rossi, M.J., Troe, J.,: Evaluated kinetic, photochemical, and heterogeneous data for atmospheric chemistry. V-IUPAC subcommittee on gas kinetic data evaluation for atmospheric chemistry. Journal of Physical and Chemical Reference Data 26, 521-1011, 1997.

Barsanti, K.C., Pankow, J.F.: Thermodynamics of the formation of atmospheric organic particulate matter by accretion reactions-part 3: carboxylic and dicarboxylic acids, Atmospheric Environment, 40, 6676-6686, 2006.

Berndt, T., Stratmann, F., Sipilä, M., Vanhanen, J., Petäjä, T., Mikkilä, J., Grüner, A., Spindler, G., Lee Mauldin III, R., Curtius, J., Kulmala, M., and Heintzenberg, J.: Laboratory study on new particle formation from the reaction OH + SO_2: influence of experimental conditions, H_2O vapour, NH_3 and the amine tert-butylamine on the overall process, Atmos. Chem. Phys., 10, 7101-7116, doi:10.5194/acp-10-7101-2010, 2010.

Bey, I., Jacob, D. J., Yantosca, R. M., Logan, J. A., Field, B. D., Fiore, A. M., Li, Q., Liu, H. Y., Mickley, L. J., and Schultz M. G.: Global modeling of tropospheric chemistry with assimilated meteorology: Model description and evaluation, J. Geophys. Res., 106(D19), 23073–23095, doi:10.1029/2001JD000807, 2001.

Bouwman, A.F., Lee, D.S., Asman, W.A.H., Dentener, F.J., Van Der Hoek, K.W., Olivier, J.G.J.: A global high-Â-resolution emission inventory for ammonia, Global Biogeochemical Cycles, 11, 561-11,587, 1997.

Bzdek, B.R., Ridge, D.P., Johnston, M.V.: Amine reactivity with charged sulfuric acid clusters, Atmos. Chem. Phys., 11: 8735–8743, doi:10.5194/acp-11-8735-2011, 2011.

Carl, S.A., Crowley, J.N.: Sequential two(blue) photon absorption by NO_2 in the presence of H_2 as a source of OH in pulsed photolysis kinetic studies: rate constants for reaction of OH with

CH_3NH_2, $(CH_3)_2NH$, $(CH_3)_3N$, and $C_2H_5NH_2$ at 295 K, Journal of Physical Chemistry A 102, 8131-8141, 1998.

Chen, M., Titcombe, M., Jiang, J., Kuang, C., Fischer, M. L., Edgerton, E., Eisele, F. L., Siepmann, J. I., Hanson, D. H., Zhao, J., and McMurry, P. H.: Acid-base chemical reaction model for nucleation rates in the polluted boundary layer, Proc. Nat. Acad. Sci., 109, 18713–18718, 2012.

De Haan, D.O., Tolbert, M.A., Jimenez, J.L.: Atmospheric condensed-phase reactions of glyoxal with methylamine, Geophysical Research Letters, 36, L11189, 2009.

Erupe, ME., Viggiano, AA., Lee, S-H.: The effect of trimethylamine on atmospheric nucleation involving H_2SO_4, Atmos. Chem. Phys., 11, 4767-4775, 2011.

Ge, X. L., Wexler, A. S., Clegg, S. L.: Atmospheric amines – Part I. A review, Atmos. Environ., 45, 524–546, 2011a.

Ge, X. L., Wexler, A.S., Clegg, S.L.: Atmospheric amines – Part II. Thermodynamic properties and gas/particle partitioning, Atmospheric Environment, 45, 561-577, 2011b.

Gibb, S.W., Mantoura, R.F.C., Liss, P.S.: Ocean-atmosphere exchange and atmospheric speciation of ammonia and methylamines in the region of the NW Arabian Sea, Global Biogeochemical Cycles, 13, 161-178, 1999a.

Grönberg, L., Lovkvist, P., Jönsson Å, J.: Measurement of aliphatic amines in ambient air and rainwater, Chemosphere, 24, 1533-1540, 1992a.

Grönberg, L., Lovkvist, P., Jönsson Å, J.: Determination of aliphatic amines in air by membrane enrichment directly coupled to a gas chromatograph, Cromatographia, 33, 77-82, 1992b.

391 Hanson, D. R., McMurry, P. H., Jiang, J., Tanner, D., Huey, L. G.: Ambient pressure proton
392 transfer mass spectrometry: detection of amines and ammonia, Environ. Sci. Technol., 45,
393 8881–8888, 2011.
394 Kurten, T., Loukonen, V., Vehkamaki, H., Kulmala, M.: Amines are likely to enhance neutral
395 and ion-induced sulfuric acid-water nucleation in the atmosphere more effectively than
396 ammonia, Atmos. Chem. Phys., 8: 4095-4103, 2008.
397 Lee, D., Wexler, A. S.: Atmospheric amines – Part III: Photochemistry and toxicity,
398 Atmospheric Environment, 71, 95-103, 2013.
399 Lloyd, J.A., Heaton, K.J., Johnston, M.V.: Reactive uptake of trimethylamine into ammonium
400 nitrate particles, Journal of Physical Chemistry A, 113, 4840-4843, 2009.
401 Murphy, S. M., Sorooshian, A., Kroll, J. H., Ng, N. L., Chhabra, P., Tong, C., Surratt, J. D.,
402 Knipping, E., Flagan, R. C., and Seinfeld, J. H.: Secondary aerosol formation from
403 atmospheric reactions of aliphatic amines, Atmos. Chem. Phys., 7, 2313-2337,
404 doi:10.5194/acp-7-2313-2007, 2007.
405 Myriokefalitakis, S., Vignati, E., Tsigaridis ,K., Papadimas, C., Sciare, J., Mihalopoulos, N.,
406 Facchini, M. C., Rinaldi, M., Dentener, F. J., Ceburnis, D., Hatzianastasiou, N., O'Dowd, C.
407 D., van Weele, M., and Kanakidou, M.: Global modelling of the oceanic source of organic
408 aerosols, Adv. Meteorol., 2010, 939171, doi:10.1155/2010/939171, 2010.
409 Nadykto, A. B., Herb, J., Yu, F., and Xu, Y.: Enhancement due to dimethylamine and large
410 uncertainties in the thermochemistry of amine-enhanced nucleation in the Earth's atmosphere,
411 Chemical Physics Letters, 10.1016/j.cplett.2014.03.036, 2014.

412 Nadykto, A. B., Yu, F., Yakovleva, M., Herb, J., and Xu, Y.: Amines in the Earth's Atmosphere:
413 A DFT Study of the Thermochemistry of Pre-Nucleation Clusters, Entropy, 13, 554-569,
414 2011.
415 Nielsen, C.J., Herrmann, H., Weller, C.: Atmospheric chemistry and environmental impact of the
416 use of amines in carbon capture and storage (CCS), Chem. Soc. Rev., 41, 6684e6704, 2012.
417 Qiu, C., and Zhang, R.: Multiphase chemistry of atmospheric amines, Phys. Chem. Chem. Phys.,
418 15, 5738–5752, 2013.
419 Qiu, Q., Wang, L., Lal, V., Khalizov, A.F., and Zhang, R.: Heterogeneous Chemistry of
420 Alkylamines on Ammonium Sulfate and Ammonium Bisulfate, Environ. Sci. Technol., 45,
421 4748–4755, 2011.
422 Schade, G.W., Crutzen, P.J.: Emission of aliphatic amines from animal husbandry and their
423 reactions: potential source of N2O and HCN, Journal of Atmospheric Chemistry, 22, 319-346,
424 1995.
425 Van Neste, A., Duce, R.A., Lee, C.: Methylamines in the marine atmosphere, Geophysical
426 Research Letters, 7, 711-714, 1987.
427 VandenBoer, T. C., Petroff, A., Markovic, M. Z., and Murphy, J. G.: Size distribution of alkyl
428 amines in continental particulate matter and their online detection in the gas and particle
429 phase, Atmos. Chem. Phys., 11, 4319-4332, doi:10.5194/acp-11-4319-2011, 2011.
430 VandenBoer, T.C., Markovic, M.Z., Petroff, A., Czar, M.F., Borduas, N., Murphy, J.G.: Ion
431 chromatographic separation and quantitation of alkyl methylamines and ethylamines in
432 atmospheric gas and particulate matter using preconcentration and suppressed conductivity
433 detection, Journal of Chromatography A, 1252, 74-83, 2012.

Wang, L., Khalizov, A. F., Zheng, J., Xu, W., Ma, Y., Lal, V., Zhang, R.: Atmospheric nanoparticle formed from heterogeneous reactions of organics, Nat. Geosci., 3, 238–242, 2010a.

Wang, L., Lal, V., Khalizov, A. F., Zhang, R.: Heterogeneous chemistry of alkylamines with sulfuric acid: implications for atmospheric formation of alkylaminium sulfates, Environ. Sci. Technol., 44, 2461–2465, 2010b.

Williams, B. J., Goldstein, A. H., Kreisberg, N. M., Hering, S. V., Worsnop, D. R., Ulbrich, I. M., Docherty, K. S., and Jimenez, J. L.: Major components of atmospheric organic aerosol in southern California as determined by hourly measurements of source marker compounds, Atmos. Chem. Phys., 10, 11577-11603, doi:10.5194/acp-10-11577-2010, 2010.

Yu, F.: A secondary organic aerosol formation model considering successive oxidation aging and kinetic condensation of organic compounds: global scale implications, Atmos. Chem. Phys., 11, 1083-1099, doi:10.5194/acp-11-1083-2011, 2011.

Yu, F., and Luo, G.: Simulation of particle size distribution with a global aerosol model: contribution of nucleation to aerosol and CCN number concentrations, Atmos. Chem. Phys., 9, 7691-7710, doi:10.5194/acp-9-7691-2009, 2009.

Yu, H., McGraw, R., and Lee S.-H.: Effects of amines on formation of atmospheric sub-3 nm particles and their subsequent growth, Geophys. Res. Lett., 39, L02807, doi: 10.1021/2011GL050099, 2012.

Zhao, J., Smith, J. N., Eisele, F. L., Chen, M., Kuang, C., and McMurry, P. H.: Observation of neutral sulfuric acid-amine containing clusters in laboratory and ambient measurements, Atmos. Chem. Phys., 11, 10823-10836, 2011.

Zollner, J. H., Glasoe, W. A., Panta, B., Carlson, K. K., McMurry, P. H., and Hanson, D. R.: Sulfuric acid nucleation: power dependencies, variation with relative humidity, and effect of bases, Atmos. Chem. Phys., 12, 4399-4411, doi:10.5194/acp-12-4399-2012, 2012.

462 Table 1. Calculated global annual mean emissions, sinks, and burdens of ammonia, MMA,
463 DMA, and TMA. Sinks and burdens under four different uptake coefficients (γ = 0.03, 0.01,
464 0.001, and 0) are given.

	γ	**Emission** (Gg N/yr)	**Oxidation** (Gg N/yr)	**Uptake** (Gg N/yr)	**Dry & Wet Deposition** (Gg N/yr)	**Burden** (Gg N)
Ammonia		5.8×10^4	-4.9×10^2	-3.8×10^4	-1.9×10^4	79.9
MMA	0.03	96.2	-17.2	-65.8	-13.2	0.07
MMA	0.01	96.2	-28.4	-48.1	-19.8	0.12
MMA	0.001	96.2	-51.7	-14.2	-30.4	0.22
MMA	0	96.2	-61.8	0.0	-34.4	0.27
DMA	0.03	38.3	-12.2	-21.9	-4.2	0.03
DMA	0.01	38.3	-17.3	-15.0	-6.0	0.05
DMA	0.001	38.3	-25.9	-3.8	-8.6	0.08
DMA	0	38.3	-28.9	0.0	-9.3	0.08
TMA	0.03	196.0	-49.8	-122.0	-23.9	0.24
TMA	0.01	196.0	-75.4	-85.7	-34.7	0.38
TMA	0.001	196.0	-122.0	-23.0	-50.9	0.63
TMA	0	196.0	-140.0	0.0	-56.2	0.72

465
466
467
468

469

470 Table 2. Available measurements of MMA, DMA, and TMA concentrations (in pptv) and site

471 information.

Site information (Latitude, Longitude)	**Site Type**	**Observation period**	**[MMA]**	**[DMA]**	**[TMA]**	**References**
A. Gothenburg, Sweden (57.73, 11.97)	Urban	Aug 24-26, 1991	3.6±0.9	0.7±0.5	1.3±0.6	Grönberg et al. (1992a)
B. Lund, Sweden (55.71, 13.19)	Urban	Jul, 1991	16±5	0.5±0.3	5.2±2	Grönberg et al. (1992b)
C. Atlanta, GA (33.85, -84.41)	Urban	6/23-8/25, 2009	<0.2	0.5 - 2	4 - 15	Hanson et al. (2011)
D. Vallby, Sweden (59.55, 17.13)	Rural	Jul, 1991	10±3	1.8±0.6	41±14	Grönberg et al. (1992b)
E. Toronto, ON (43.67, -79.39)	Rural	6/27-7/5, 2009		0.2 – 2.5		VandenBoer et al. (2011)
F. Egbert, ON (44.23, -79.79)	Agricultural and semi-forested	10/15-11/2, 2010		6.5±2.1	1.0 - 10	VandenBoer et al. (2012)
G. Coastal Sweden (Malmö) (55.62, 13.00)	Coast	Aug 13-15, 1991	4.4±1.1	1.1±0.4	8.7±3.1	Grönberg et al. (1992a)
H. Oahu, Hawaii (21.48, -158.00)	Coast	Jul-Aug, 1985	0.2±0.1	2.0±1.1	0.7±0.4	Van Neste et al. (1987)
I. Narragansett, Rhode Island (41.45, -71.45)	Coast		1.2±0.3	5.3±0.9	2.2±0.9	Van Neste et al. (1987)
J. Arabian Sea (14, 63)	Arabian Sea	8/27-10/4, 1994	2.5	0.9	0.02	Gibb et al. (1999)
K. Arabian Sea (14, 63)	Arabian Sea	11/16-12/19, 1994	3.2	4.4	0.2	Gibb et al. (1999)
L. NW Atlantic (13.2, -66.1)	Marine	2/28/1986	0.33			Mopper and Zika (1987)

472

473

474

Figure Captions

Figure 1. Horizontal distributions of annual mean DMA emissions assumed in the present study.

Figure 2. Simulated horizontal distributions of annual mean DMA oxidation and uptake lifetime and concentration ([DMA]) in the model surface layer (0 – 150 m above surface) under two aerosol uptake coefficients: (a-b) γ=0 (i.e., oxidation only) and (c-d) γ=0.03 (uptake by sulfuric acid particles).

Figure 3. Same as Fig. 2 but for zonally averaged values. Vertical axis is the ratio of pressure (P) at the model layer to the pressure at the surface (P_{surf}).

Figure 4. Horizontal distributions of [MMA] in the surface layer (a, c) and its zonally averaged values (b, d) under two different uptake coefficients (γ = 0.03, and 0).

Figure 5. Same as Figure 4 except for [TMA].

Figure 6. A comparison of simulated and measured [MMA], [DMA], and [TMA] at the sites listed in Table 2 and marked in Fig. 1 by letters. Model results correspond to the months of the observations, and vertical bars define the simulated ranges of monthly mean values.

Fig 1

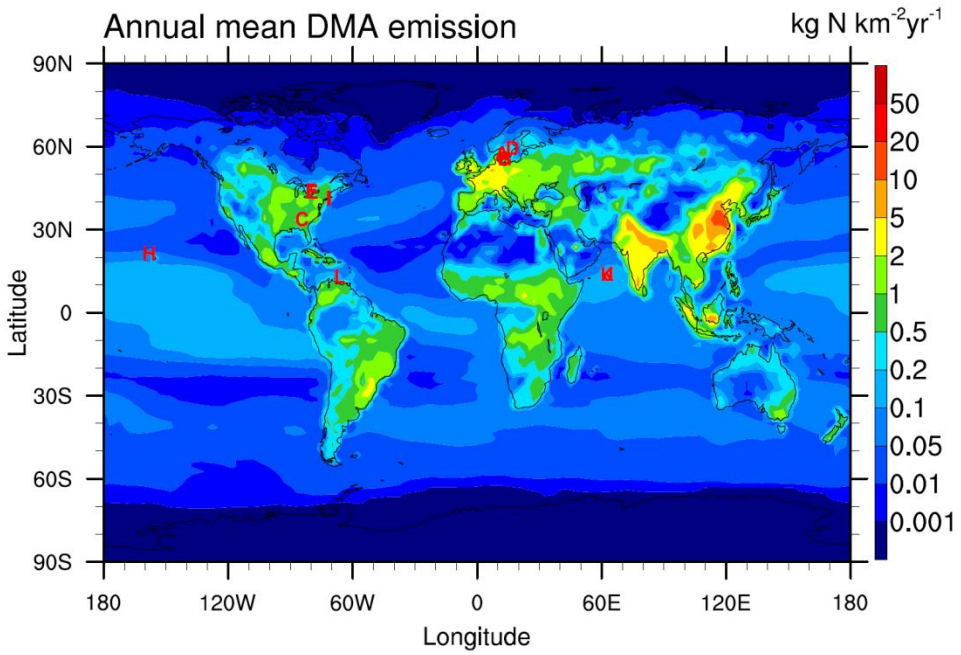
Annual mean DMA emission
kg N km-2yr-1
50
20
10
5
2
1
0.5
0.2
0.1
0.05
0.01
0.001
90N
60N
30N
0
30S
60S
90S
Latitude
180
120W
60W
0
60E
120E
180
Longitude
A
B
C
D
E
F
G
H
I
J
K
L

Fig 2

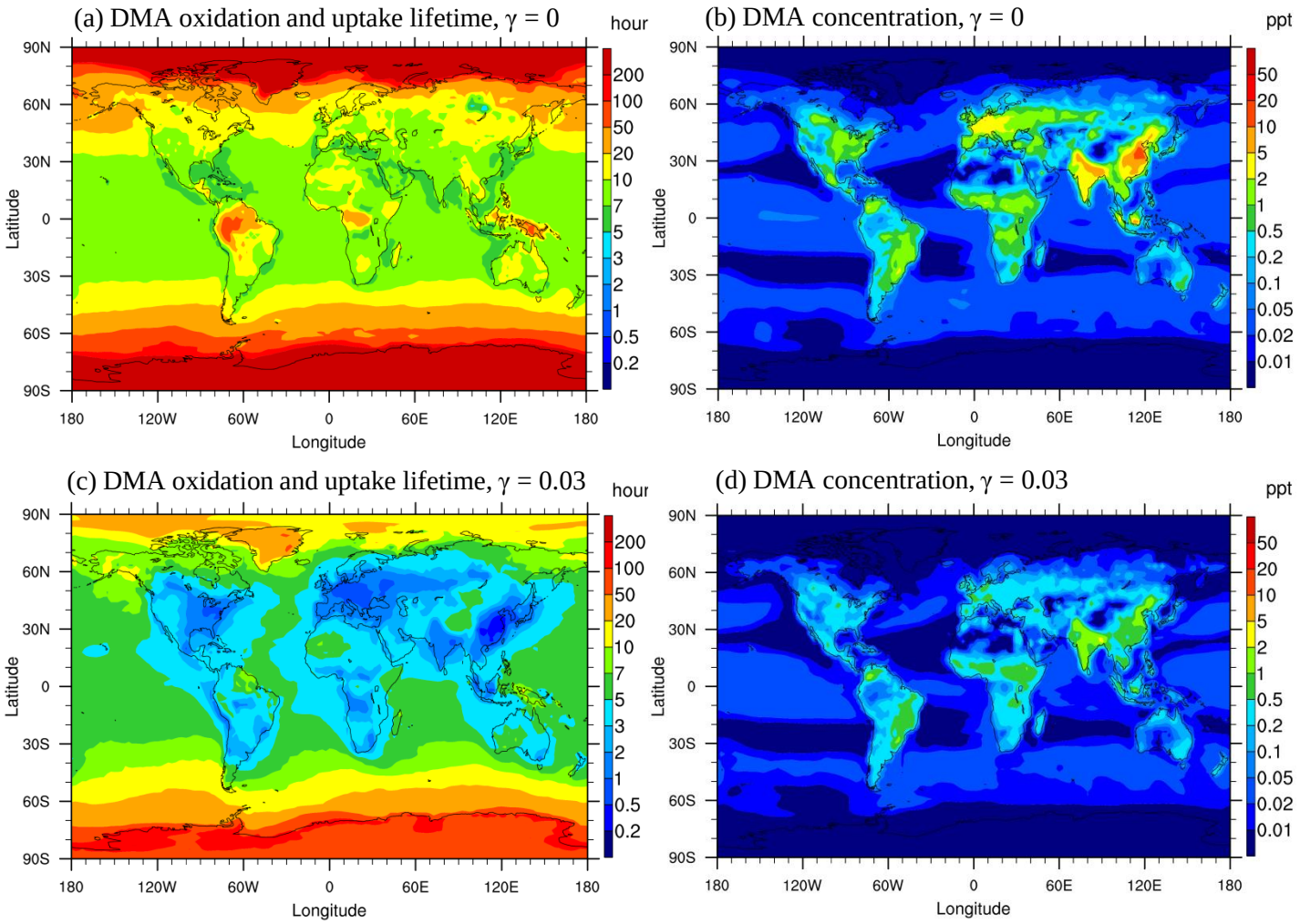
(a) DMA oxidation and uptake lifetime, γ = 0
hour
200
100
50
20
10
7
5
3
2
1
0.5
0.2
90N
60N
30N
0
30S
60S
90S
Latitude
180
120W
60W
0
60E
120E
180
Longitude
(b) DMA concentration, γ = 0
ppt
50
20
10
5
2
1
0.5
0.2
0.1
0.05
0.02
0.01
(c) DMA oxidation and uptake lifetime, γ = 0.03
(d) DMA concentration, γ = 0.03

Fig 3

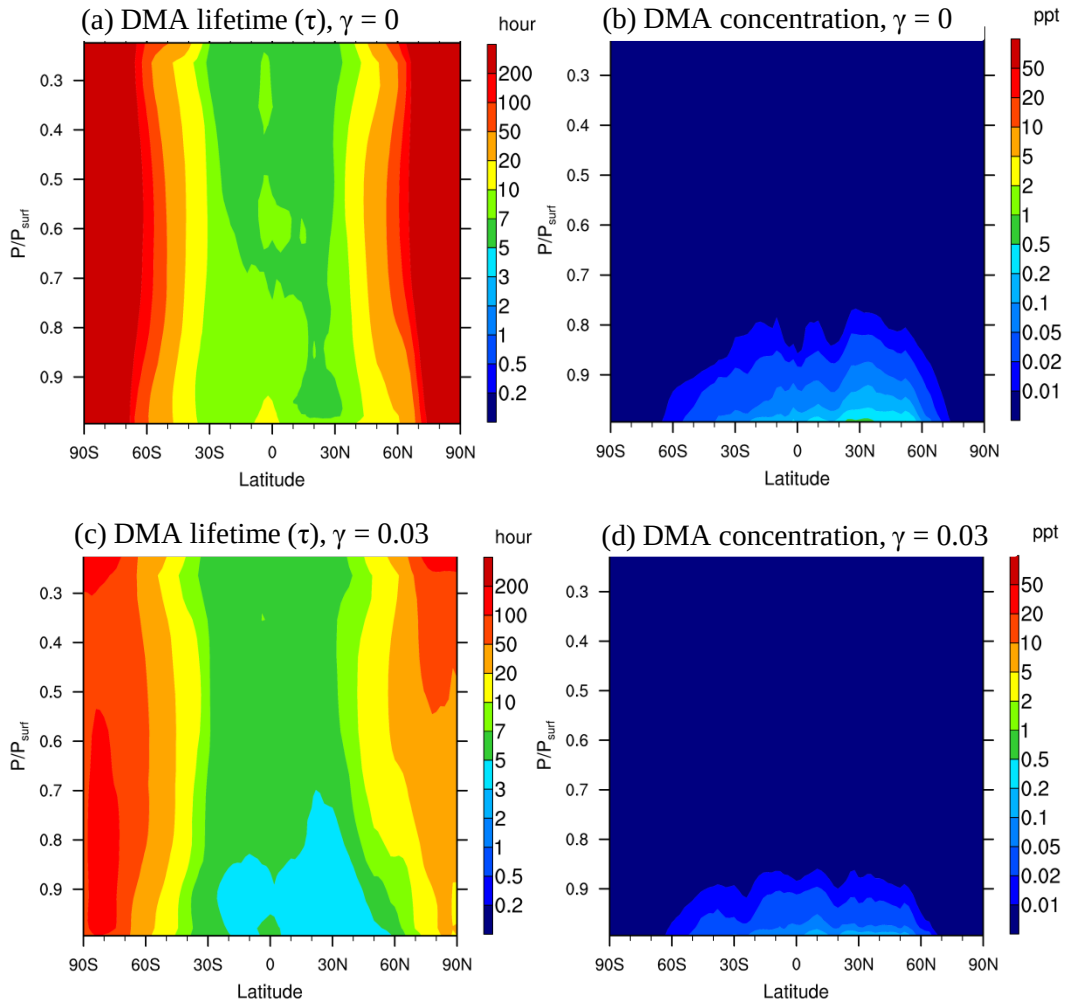
(a) DMA lifetime (τ), γ = 0
hour
200
100
50
20
10
7
5
3
2
1
0.5
0.2
(b) DMA concentration, γ = 0
ppt
50
20
10
5
2
1
0.5
0.2
0.1
0.05
0.02
0.01
(c) DMA lifetime (τ), γ = 0.03
(d) DMA concentration, γ = 0.03
P/P_surf
0.3
0.4
0.5
0.6
0.7
0.8
0.9
90S
60S
30S
0
30N
60N
90N
Latitude

Fig 4

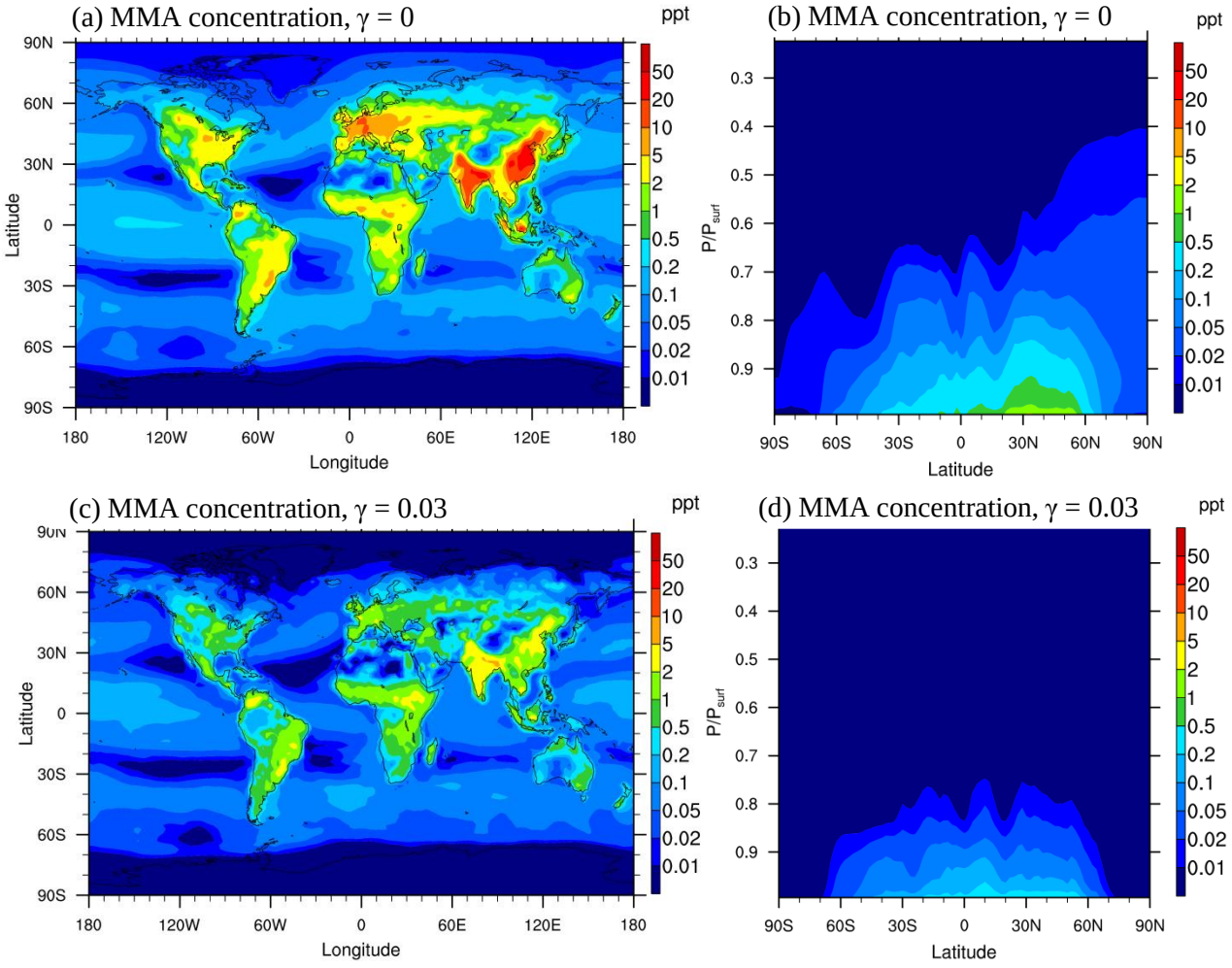
(a) MMA concentration, γ = 0
ppt
50
20
10
5
2
1
0.5
0.2
0.1
0.05
0.02
0.01
90N
60N
30N
0
30S
60S
90S
Latitude
180
120W
60W
0
60E
120E
180
Longitude
(b) MMA concentration, γ = 0
ppt
P/P_surf
0.3
0.4
0.5
0.6
0.7
0.8
0.9
90S
60S
30S
0
30N
60N
90N
Latitude
(c) MMA concentration, γ = 0.03
ppt
Latitude
Longitude
(d) MMA concentration, γ = 0.03
ppt
P/P_surf
Latitude

Fig 5

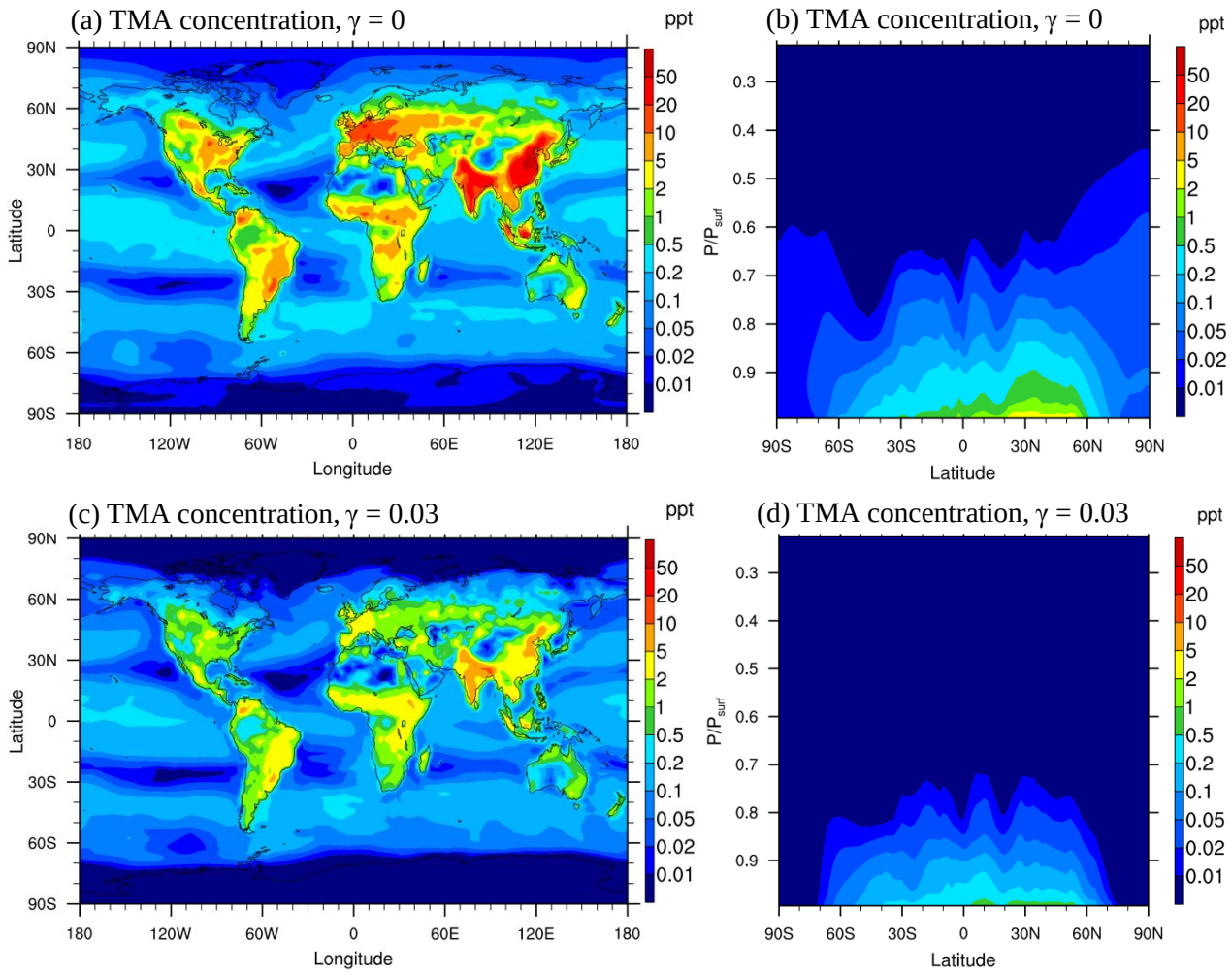
(a) TMA concentration, γ = 0
ppt
50
20
10
5
2
1
0.5
0.2
0.1
0.05
0.02
0.01
90N
60N
30N
0
30S
60S
90S
Latitude
180
120W
60W
0
60E
120E
180
Longitude
(b) TMA concentration, γ = 0
ppt
0.3
0.4
0.5
0.6
0.7
0.8
0.9
P/P_surf
90S
60S
30S
0
30N
60N
90N
Latitude
(c) TMA concentration, γ = 0.03
ppt
(d) TMA concentration, γ = 0.03
ppt

Fig 6

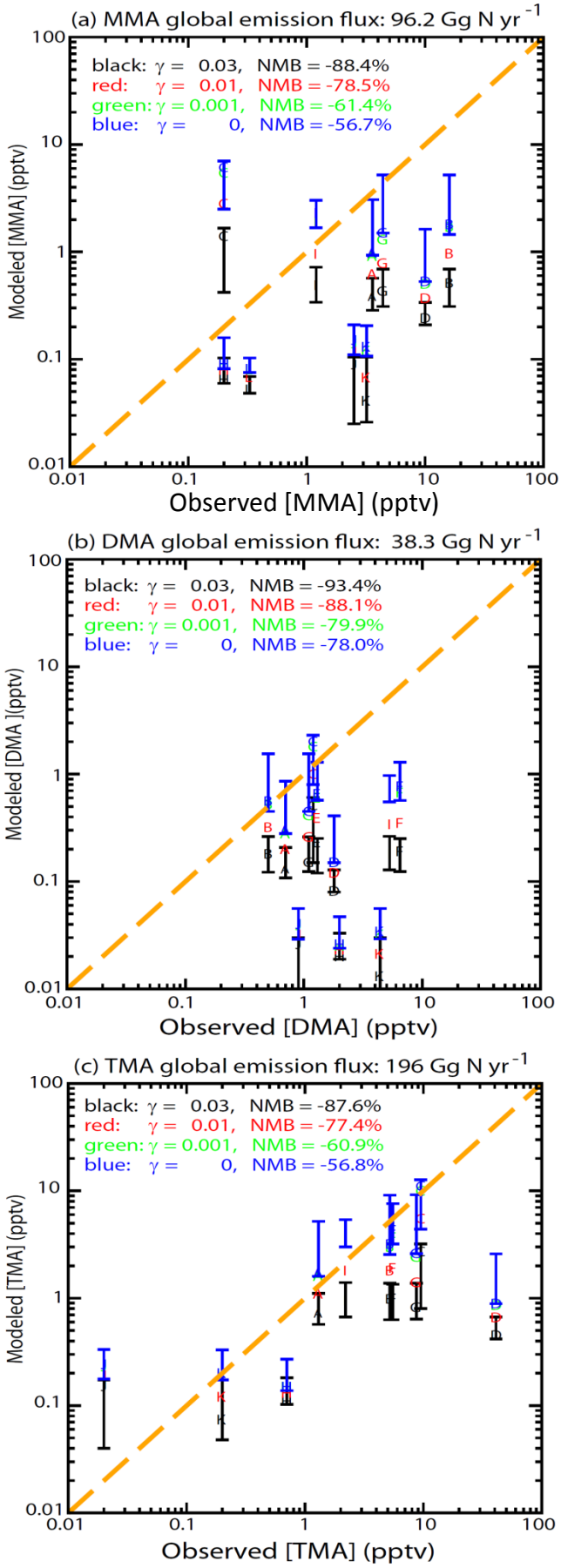
(a) MMA global emission flux: 96.2 Gg N yr -1
black: γ = 0.03, NMB = -88.4%
red: γ = 0.01, NMB = -78.5%
green: γ = 0.001, NMB = -61.4%
blue: γ = 0, NMB = -56.7%
Modeled [MMA] (pptv)
Observed [MMA] (pptv)
(b) DMA global emission flux: 38.3 Gg N yr -1
black: γ = 0.03, NMB = -93.4%
red: γ = 0.01, NMB = -88.1%
green: γ = 0.001, NMB = -79.9%
blue: γ = 0, NMB = -78.0%
Modeled [DMA](pptv)
Observed [DMA] (pptv)
(c) TMA global emission flux: 196 Gg N yr -1
black: γ = 0.03, NMB = -87.6%
red: γ = 0.01, NMB = -77.4%
green: γ = 0.001, NMB = -60.9%
blue: γ = 0, NMB = -56.8%
Modeled [TMA] (pptv)
Observed [TMA] (pptv)
0.01
0.1
1
10
100